The quantification of entropy for multicomponent systems: application to microwave-assisted comminution

Belo Fernandes, I.; Rudolph, M.; Hassanzadehmahaleh, A.; Bachmann, K.;
Meskers, C. E. M.; Peuker, U.; Reuter, M.;

Originally published:

August 2021

Minerals Engineering 170(2021), 107016

DOI: https://doi.org/10.1016/j.mineng.2021.107016

The quantification of entropy for multicomponent systems: application to microwave-assisted comminution

I. B. Fernandes [a,b,*]; M. Rudolph [a]; A. Hassanzadeh [a]; K. Bachmann [a] , C. Meskers [a]; U. Peuker [b]; M.A. Reuter [a, c]

[a] Helmholtz-Zentrum Dresden-Rossendorf, Helmholtz Institute Freiberg for Resource Technology, Chemnitzer Straße 40, 09599 Freiberg, Germany

[b] Institute of Mechanical Process Engineering and Mineral Processing, Technische Universität Bergakademie Freiberg, Germany, Agricolastraße 1, 09599 Freiberg, Germany

[c] SMS group GmbH, Ivo-Beucker-Straße 43, 40237 Düsseldorf, Germany

[*] Corresponding author: I. B. Fernandes, email: i.fernandes@hzdr.de

Abstract

The second law of thermodynamics, through exergy analysis, is commonly applied to quantify process inefficiencies in metallurgical reactors, however, it is not yet being used to understand physical processes and changes in particle-based systems. Correlating the state of mixing of particle texture and homogeneous liquid mixtures is of importance. This paper applies the exergy analysis and excess entropy method to two sets of experiments highlighting the differential breakage as microwave pre-treatment is applied to a gold-copper ore. Grinding kinetic properties were measured following the top-size fraction method and calculated using the population balance model. The approach combines the mixing entropy on the system level (streams) and the entropy for multicomponent particle systems, using automated mineralogy data to quantify the effects of intergrowth and improvements in grinding performance. This is a first step towards understanding mineral processing not only in terms of energy conservation (first law of thermodynamics) but also in terms of the quality of energy available at multicomponent systems (second law of thermodynamics). When applied to comminution processes, this methodology enables us to understand the change in particle composition (its degree of liberation) as well as changes in particle size, being an important measure of process efficiency and selectivity.

Keywords:

Excess entropy analysis, exergy distribution, mineral liberation, microwave-assisted breakage, grinding kinetics

1. Introduction

Energy consumption is a critical aspect of minerals processing and metallurgy and it plays a major role in the environmental impact when looking at large production systems (Abadias Llamas *et al*. 2019; Fernandes, Abadías Llamas, and Reuter 2020). Comminution processes alone consume over 35% of the total energy used in a mining operation (Ballantyne and Powell 2014; Curry, Ismay, and Jameson 2014), being a key aspect in the economic and environmental performance of any operation. As the mineral industry moves towards processing low-grade and more complex ores, there is an increasing need to improve the energy efficiency of comminution processes and reduce its power consumption.

Complex ores often require longer grinding times to liberate the intergrown mineral phases so that they are concentrated and readily accessible for metallurgical processing. Therefore, metallurgists and mineral processing experts must find a common measure to address process efficiency, correlating the state of mixing of particle texture and homogeneous liquid mixtures (Peuker *et al*. 2021).

Gay (2004) states that the relationship between the feed and product particles can be estimated using a probability method, based on the concept that the distribution is at maximum randomness, subject to mass and composition constraints. This can be applied for chemical transformation processes, as well as physical separation and particle liberation processes.

Losses generated as a result of entropy gain in the system are represented by internal exergy, whereas loss of matter, heat, and radiation are related to external exergy. The total exergy (E) of a stream is defined as the maximal amount of work, or useful energy, that can be obtained from it as it reaches equilibrium with the environment (Szargut 1989), being determined as the sum of its physical and chemical exergy (Abadias Llamas *et al*. 2019).

$$E = \Delta H - T\Delta S + \sum n_i . e^0{}_i \quad (1)$$

where ΔH, in kJ, denotes the standard enthalpy of the system, representing the energy input into the system; ΔS denotes the entropy, in J/K; *T* is the temperature of the system, in K; n_i is the number of moles of component *i*, and $e^0{}_i$ is the chemical exergy of component *i*, in kJ/mol.

The physical exergy remains constant in a comminution process, as there are no changes in temperature and pressure. The chemical exergy of a material stream (e_{ch}) is calculated as the sum of standard chemical exergies of each component *i* ($e^0{}_i$) and the relative increase in entropy due to mixing (Amini *et al*. 2007; Ignatenko, van Schaik, and Reuter 2007):

$$e_{ch} = \sum_i n_i \cdot e^0{}_i + RT_0 n \sum_i y_i \cdot lny_i \quad (2)$$

where y_i is the molar concentration of component *i*, *n* is the total number of moles in the mixture, *R* is an energetic factor (ideal gas constant, 8.314 J/mol.K).

The first term of Eq. 2 shows that exergy considers the mass/composition of a material and the second term quantifies its quality due to mixing (Meskers *et al*. 2008). Exergy efficiency has been successfully applied to separation processes (Velázquez Martínez *et al*. 2019), describing the entropy of mixtures at different streams to evaluate its separation efficiency, and to understand large systems (Abadias Llamas *et al*. 2019; Fernandes *et al*. 2020), describing the exergy destruction along a complex value chain. However, there is still a lack of understanding of the entropic effects on a particle level and its state of intergrowth. An understanding of breakage looking at multicomponent systems, on the particle level, would enable us to quantify and improve the performance of existing technologies, in particular looking at mineral selectivity for grinding and energy efficiency.

Pre-treatment technologies, such as microwave dielectric heating, high voltage electrical pulse, or chemical treatments (Adewuyi *et al*. 2020) help induce differential breakage and reduce the energy required for comminution (Haque 1999). In this paper, microwave pre-

treatment is used to evaluate the grinding behaviors of ores and showcase the applicability of the entropy analysis for the assessment of comminution processes.

The development of microwave heating of rocks (Wong 1975) occurred as the industry observed that common heating mechanisms such as convection, conduction, and radiation are slow and generate low crack density in the matrix, resulting in non-selective heating of the target mineral phases (Somani *et al*. 2017). The majority of naturally occurring ores have varying thermal properties, resulting in varying degrees of thermal expansion for each mineral due to differential stress created within the lattice, which in turn results in the generation of micro-cracks and the development of intergranular and/or intragranular fractures (Leißner *et al*. 2016), with potential to improve the liberation degree of the target mineral. Sulfides and oxides have the largest range of variation of dielectric constants (Cao 2012), while quartz and other major rock-forming minerals are very poor absorbers of microwave energy (Jinkai 1990; John *et al*. 2015).

Batchelor *et al*. (2016), Bobicki, Liu, and Xu (2014), Gholami *et al*. (2020a), and Lu *et al*. (2017) showed that the heating characteristics of different ore types are dependent on their mineralogy, preferably when strong microwave-absorbing minerals are found within a hard matrix, such as quartz or feldspars (Batchelor *et al*. 2015). The hard matrix avoids elastically absorbing the thermal expansion, which builds up tension within the particles. Microwave-treatment of rocks generates a thermal signature that could be used to sort ore particles and avoid overgrinding gangue particles (Bobicki *et al*. 2020). Furthermore, it was reported that microwave-treatment is not detrimental to the flotation of sulfides (Gholami *et al*. 2020b).

The use of microwaves to selectively heat minerals has been extensively studied in the literature. Therefore, the focus of this paper is shifted towards a grinding kinetics perspective for a complex gold-copper ore. The improvements observed in microwave-treatment are linked to the entropy analysis for size reduction processes. The differential heating behavior on microwave pretreatment is used to showcase the entropy analysis for size reduction processes and analyze the exergy distribution on different liberation classes, looking at multicomponent systems and understanding the entropy creation potential as grinding takes place.

2. Theoretical background

2.1. Excess entropy for intergrown particles

Peuker *et al*. (2021) introduce the concept of molar excess entropy, $\bar{S}^x$, which takes into account the structure of a disperse system consisting of intergrown particles, therefore adding the microscopic level effects to Eq. 2. The excess entropy increases the complexity of a system by taking into account not only particle size but also particle texture, through an understanding of the state of intergrowth at the microscale, for each component *i* and particle *j*:

$$n \cdot \bar{S}^x = -n Ł \sum_i y_i \cdot ln y_i = -\sum_j n_j Ł \sum_i z_{i,j} ln\, z_{i,j} \qquad (3)$$

where Ł represents an entropy creation factor for a specific size reduction process, measured in J/K, and $z_{i,j} = \frac{n_{i,j}}{n_j}$ represents the molar concentration of component i in particle j.

$$\bar{S}^x = -Ł \sum_j \sum_i \frac{n_{i,j}}{n} ln \frac{n_{i,j}}{n_j} \qquad (4)$$

As the value for the Ł is unknown, the dimensionless molar excess entropy factor ($\frac{\bar{S}^x}{Ł}$) is used for quantification of excess entropy change during comminution:

$$\frac{\bar{S}^x}{Ł} = -\sum_j \sum_i \frac{n_{i,j}}{n} ln \frac{n_{i,j}}{n_j} \qquad (5)$$

Considering that the macroscale represents the chemical exergy of each mineral separately, and it remains unchanged during comminution as there is no chemical transformation in the system, the first term in Eq. 2 can be neglected. Therefore, any change in entropy ($\Delta\bar{S}$) during comminution is related to the mixing effect at meso (ideal state of mixing within the system) and micro (mixing on particle level) scales.

$$\frac{\Delta\bar{S}}{Ł} = \sum_i y_i \cdot lny_i + \sum_j \sum_i \frac{n_{i,j}}{n} ln \frac{n_{i,j}}{n_j} \qquad (6)$$

The estimation of the entropy creation factor Ł is still a challenge and should be addressed in further studies (Peuker *et al*. 2021).

2.2. Population balance model

The population balance model is referred to as a simple mass balance for the size reduction process, controlling the particle size distribution and determining the breakage mechanisms during comminution (Herbst 1979). The population balance method considers size reduction as two components of fracture: a fracture event, characterized by the breakage distribution function; and a fracture process, represented by the kinetics or selection function (Kelly and Spottiswood 1990).

The primary breakage distribution function represents the cumulative weight fraction of the material broken from size *j* into smaller size intervals *i*, being represented as B_{ij}. The distribution is ideally measured before any fragment is reselected for further breakage, characterizing primary breakage (Austin and Luckie 1972).

The primary breakage distribution function can be determined from single-size-fraction experiments at short grind times. It has been observed that B_{ij} values are often insensitive to milling conditions. Austin *et al*. (1984) developed an empirical equation relating the cumulative breakage function B_{ij} and particle size:

$$B_{ij} = \Phi \left(\frac{d_{i-1}}{d_j}\right)^{\gamma} + (1-\Phi)\left(\frac{d_{i-1}}{d_j}\right)^{\beta}, \; 0 < \Phi < 1; i > j \qquad (7)$$

where d_j is the top particle size, d_i is the particle size at size interval *i*, and Φ, γ, and β are dependent on the material. Φ represents the fraction of fines produced in a single fracture event, whereas γ is the slope of the fine grinding term and β is the slope of the coarser grinding term. Typical values for γ range from 0.6-1.3 and β from 2.5 to 5.

B_{ij} values can be obtained by back-calculation using the BII method (Austin and Luckie 1972):

$$B_{i,1} = \frac{log[(1-P_i(0)) \,/\, (1-P_i(t))]}{log[(1-P_2(0) \,/\, (1-P_2(t))} \qquad (8)$$

where P_i(t) is the cumulative mass fraction less than size interval *i* at time *t*. $B_{i,1}$ is the cumulative mass fraction of particles passing the top size interval *i* from breakage of particles of size *j*=1 (top size). $P_2(0)$ represents the sieving error, being the mass fraction passing the top size fraction and it should be less than 5%.

The kinetics of breakage or rate of disappearance represents the probability of a specific particle for being selected for breakage. It is dependent on the milling equipment, operating conditions, and particle size. If S_1 does not vary with time (first-order grinding), it can be calculated from Eq. $w_1(t) = w_0 exp^{-S_1 t}$ (9**Error! Reference source not found.** following the one-size-fraction technique:

$$w_1(t) = w_0 exp^{-S_1 t} \qquad (9)$$

where S_1, in min^{-1}, is the specific rate of breakage or selection function and w_i(t) is the mass fraction in size class *i* at time *t*.

Austin *et al*. (1984) developed a model for the specific rate of breakage defined in relation to particle size:

$$S_i = \frac{a\left(\frac{di}{dj}\right)^{\alpha}}{1+\left(\frac{di}{\mu}\right)^{\lambda}} \qquad (10)$$

The characteristic diagram for Austin function shows that the breakage kinetics is at maximum for a size that is slightly less than μ and that it then decreases towards both the fine and coarse side of the particle population. Parameter a represents the breakage rate constant, being directly proportional to the specific rate of breakage. α is related to finer particle sizes whereas λ represents the deceleration rate after the inflection point for coarser particle sizes.

3. Design of experiments

3.1. Sampling, preparation and characterization

Samples for this study are originated from the Buzwagi orogenic gold-copper deposit, collected by Wikedzi (2018) and used for determination of the Bond work index, breakage kinetics, and liberation characteristics (Wikedzi *et al*. 2020). Additional information regarding the deposit, grinding circuit, and concentration process can be obtained from Wikedzi (2018).

47 kg of samples in size -250 mm were crushed to -5mm then dry sieved to collect material in the following single-size fractions: -1600+1250 µm, -1250+9000 µm, -850+500 µm, -425+315 µm, -315+200 µm, and -212+160 µm. The American Standard Test Sieve Series (ASTM) was used. Representative samples of approximately 750 g were obtained and used for grinding kinetics experiments according to the *single-size fraction* technique (Austin *et al*., 1984).

Table 1 presents the experimental design for grinding kinetics experiments, showing the microwave exposure time and sieves used for each *single-size fraction* experiment. The size fractions selection was done based on the final intended target grinding size at the mine site, to reach p_{80} of approximately 125 µm and gather sufficient and reliable automated mineralogy data.

Table 1. One-size fraction breakage technique for BII method: single-size fractions used

Single-size fraction test (µm)	Sieve sizes (µm)												Microwave-treatment time (s)
	1250	900	600	500	315	250	160	125	90	63	50	36	
-1600 +1250													0, 30, 60, 90, 120
-1250 +900													0
-850 +500													0, 30, 60, 90, 120
-425 +315													0, 120
-315 +212													0
-212 +160													0

3.2. Comminution experiments

Considering the limited amount of sample material within each size fraction and the need to run duplicate tests at different microwave-exposure times, a standard Bond ball mill could not be used to perform breakage function comminution tests. Therefore, a smaller ball mill was used in this study, resembling the milling conditions within a Bond ball mill.

It is important to mention that the breakage function is material-dependent only, whereas the kinetics of breakage (selection function) is influenced by the milling equipment of choice. Microwave treatment would, therefore, affect the material properties and influence the

breakage distribution function. The mill, media, and ore characteristics are displayed in Table 2. The distribution of balls and amount of ore was selected in order to simulate the conditions in a Bond test, in terms of fractional ball filling, fractional powder filling, and proportion of ore to grinding media.

Table 2. Detailed information regarding the ball mill, media charge, and ore characteristics

Milling equipment	Diameter (mm)	215
	Length (mm)	165
	Volume (L)	6
	Critical speed (rpm)	91.2
	Power (W)	360
Grinding media	Material	Stainless steel
	Specific gravity (g/cm^3)	7.81
	Diameter (mm)	21 (90 balls)
		18 (110 balls)
		15 (130 balls)
	Total media mass (kg)	7.83
	Fractional ball filling, J_c (%)	16.70
Ore	Specific gravity (g/cm^3)	2.8
	Total material mass (g)	750
	Fractional powder filling, f_c (%)	7.4
	Bond work index, W_i (kWh/t) (Wikedzi *et al*. 2018)	17.20
	Ratio ore:grinding media (vol %)	21.0

Microwave pre-treatment was performed using a 1050W SHARP R-941STW domestic microwave oven, with an operating frequency of 2.45 GHz, at 100% power and cavity dimensions of 375mm (W) x 272mm (H) x 395mm (D). 750g of each sample were spread evenly on a ceramic turntable of 362mm diameter. To establish microwave-dependent graphs, ore samples were exposed to microwave radiation for different increments of time: 30, 60, 90, and 120 s (Table 1). The input power for this device is 1340W.

Grinding was performed at short intervals, aiming at avoiding re-breakage. The cumulative grinding time for each test was 10, 20, 40, 80, 120, and 240 s. The particle size distribution was obtained by sieving for the feed and at every grinding step, having in total seven size analyses for each test. Representative samples were taken and sent for X-ray fluorescence (XRF), X-ray diffraction (XRD), and mineral liberation analysis (MLA) to measure the ore variability at different grinding intervals.

3.3. Mineral liberation analysis

Samples were prepared using material from four sets of experiments: at top size fraction -1600+1250 µm and -425+315 µm, for an ore subjected to microwave treatment for 120 s and untreated ore. Six samples were collected for each experiment (after 0, 20, 40, 80, 120, 240 s grinding), having a total of 22 MLA samples (Figure 1). Crosscut grain mounts were prepared using aliquots of 3 g of material, mixed with graphite and epoxy resin, according to (Heinig *et al.* 2015). The grain mounts were polished and carbon-coated. The samples were analyzed by a Mineral Liberation Analyzer (MLA), comprising a FEI Quanta 650F field emission scanning electron microscope (SEM) equipped with two Bruker Quantax X-Flash 5030 energy-dispersive X-ray detectors (EDX). Back-scattered electrons (BSE) are used for image segmentation and EDX-spectra for mineral classification. The grain-based x-ray mapping (GXMAP) measurement mode was selected for analysis of the sample and sparse phase liberation (SPL) mode was selected for the identification of sulfide phases. More detailed information about the functionality of MLA and offline processing of the data can be found in Fandrich *et al.* (2007) and Bachmann *et al*. (2017). Basic particle data processing was

performed with the software package MLA Dataview 3.1.4.686 and MATLAB R2020a was used to incorporate the concepts of excess entropy and exergy to the particle data.

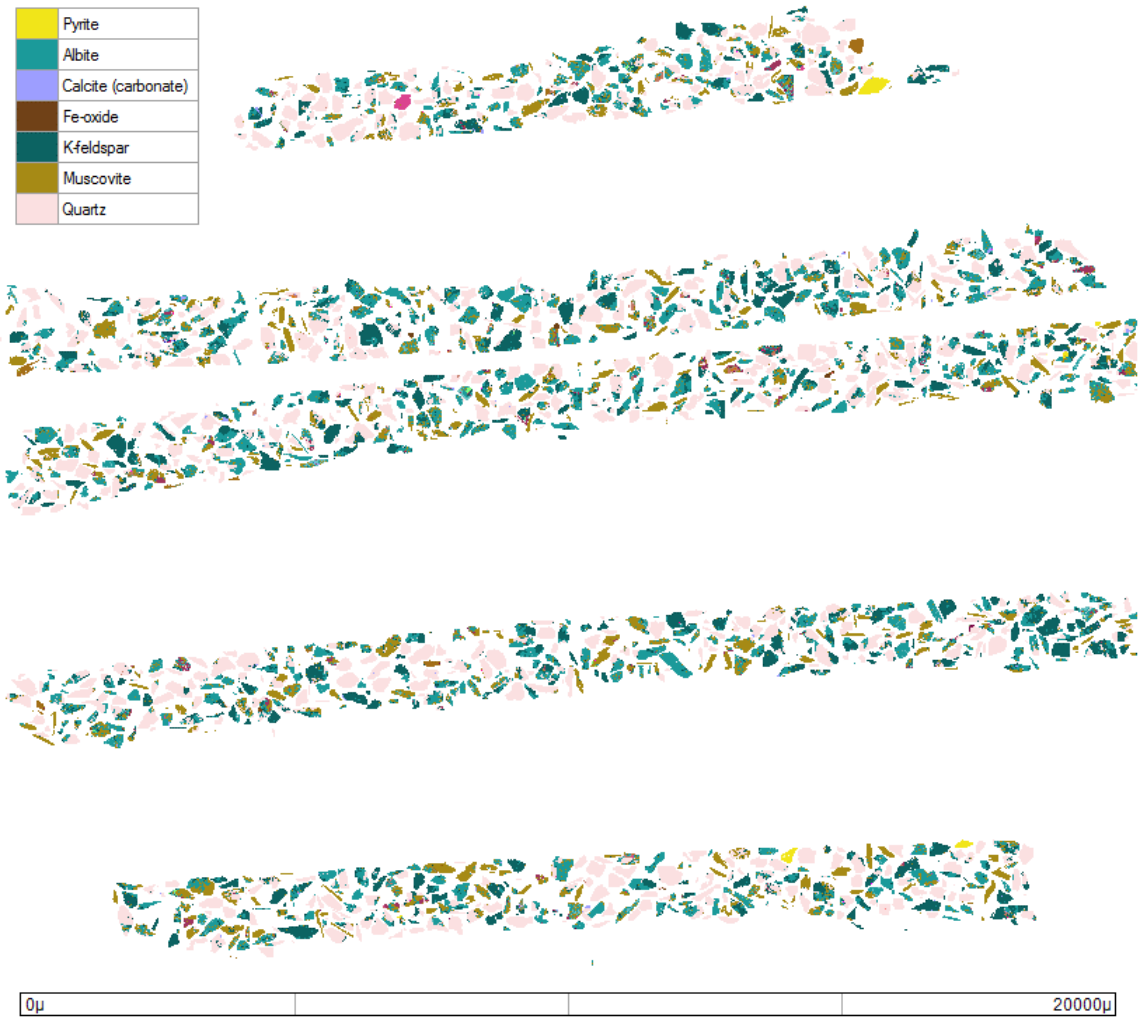

Figure 1. Mineral liberation analysis image from the feed sample (experiment on top size fraction -425+315 µm). 52 particles containing sulfide minerals (in yellow) were found in this sample (out of 5233 particles in total). Major minerals are shown in the legend

4. Results and discussions

4.1. Size reduction and liberation: Untreated ore vs microwave-treated ore

Fracture along grain boundaries can be induced when microwave-absorbing minerals are found within a matrix of hard microwave-transparent minerals and subjected to high microwave power (Batchelor *et al*. 2015, 2016; Bobicki *et al*. 2014; S. W. Kingman *et al*. 2004; S.W. Kingman *et al*. 2004). Figure 2 shows the mineralogical composition of the ore, having 0.78% sulfides (strong microwave-absorbers) and 0.61% oxides (poor microwave-absorbers) in a matrix composed mostly of quartz, feldspars, and mica minerals (mostly muscovite) as microwave-transparent gangue. It presents the grouped modal mineralogy of the sample represented in Figure 1.

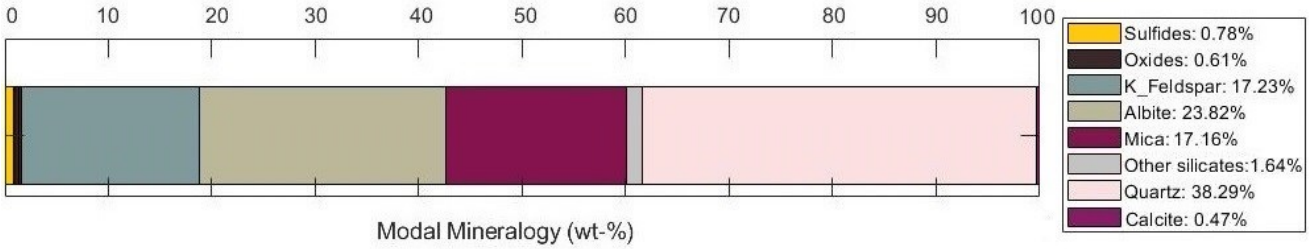

Figure 2. Modal mineralogy of the feed sample. Pyrite is the predominant mineral in the sulfides group. Iron oxides and titanite represent the oxides group. Muscovite and biotite represent the mica group. Other silicates are mostly composed of epidote and chlorite.

It is well known that rocks break more easily by tension than compression stress. Sulfides have a high microwave absorption rate, leading to thermal expansion and increased tension in the grain boundaries, which can induce the formation of microcracks (Lu *et al*. 2017; Wang *et al*. 2008). The particle size distribution after 240 s grinding time is shown in Figure 3, for untreated and microwave-treated samples. Improvements in size reduction can be observed at microwave exposure times of over 90 s.

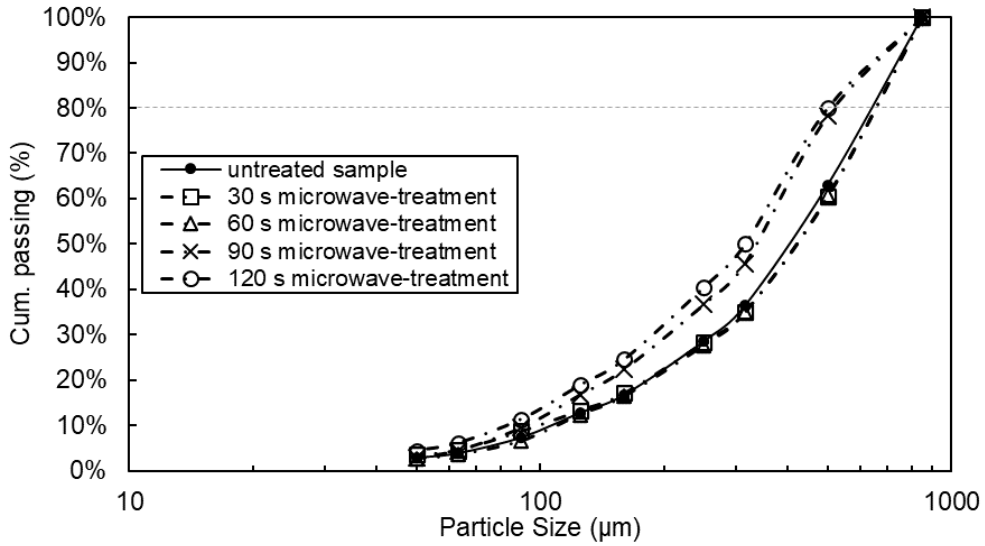

Figure 3. Cumulative particle size distribution after 240 s grinding for varying microwave exposure times: 0, 30, 60, 90, and 120 s. Top size fraction: -800+500 µm. The horizontal gray line is used to guide the eye towards the p80 for each sample

Thus, experiments on ore exposed to microwaves for 120 s were selected for mineral liberation analyses to observe higher contrasts between grinding experiments on untreated and microwave-treated samples. Figure A. 1, in the appendix, presents the cumulative size distribution from MLA data obtained from experiments on top size fractions -1600+1250 µm and -425+315 µm. It shows that microwave treatment aids in breakage by having smaller particle sizes for the same grinding time.

However, reaching finer particle sizes does not necessarily mean that comminution is more efficient. Mineral liberation is a more relevant indicator of comminution efficiency than size reduction, as correctly stated by Little *et al*. (2016). It is important to understand whether it is possible to reach similar liberation characteristics at shorter grinding times. Figure 4 presents the cumulative mass recovery for different minerals (sulfides, micas, feldspars, and quartz) at each liberation class.

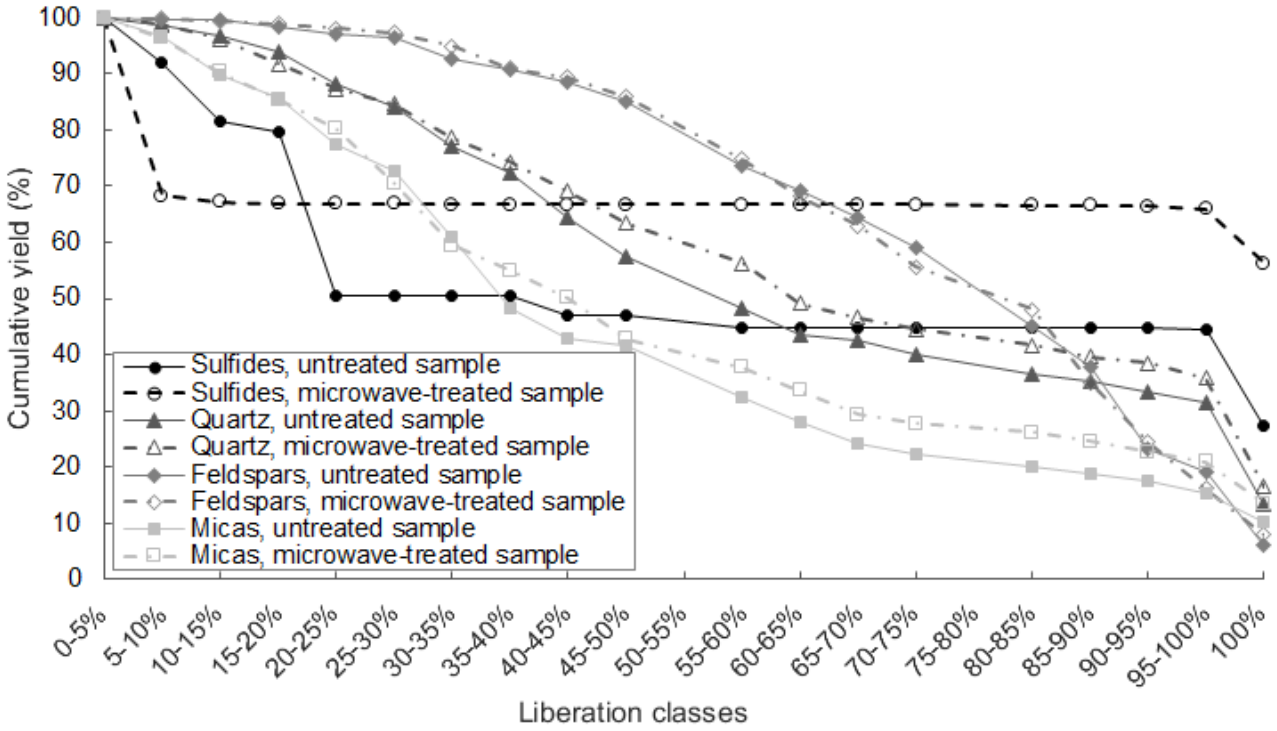

Figure 4. Cumulative liberation for different minerals (sulfides, micas, feldspars, and quartz) for untreated and microwave-treated samples, after 240 s grinding from comminution experiment on top size fraction -1600+1250µm

It becomes clear that microwave-treatment improves the liberation degree of the sulfides, as the amount of fully liberated particles increases from 27% to 56% after microwave-treatment, whereas for gangue minerals no significant differences are observed. It can be also observed a bimodal distribution of sulfide minerals, being concentrated either in liberated classes (>90%) or in low liberation classes (<20%). This behavior might be explained due to the porphyritic characteristic of the ore, presenting coarse sulfide grains within a matrix of fine particles, and fine-grained sulfides. A similar pattern is observed in Figure 5, showing the cumulative grain size distribution for pyrite (mineral of interest) and quartz (representing main gangue mineral) after 120 s and 240 s grinding. Despite the overall reduction in particle size when microwave treatment is applied to the ore (see Figure 3), the mineral grain size distribution for sulfides is coarser when compared to the untreated samples, meaning that improvements in breakage mechanism are observed, leading to fewer transgranular breakage. For quartz, no distinct differences are observed for microwave-treated and untreated samples, which demonstrates that microwave treatment selectively enhances the liberation of sulfide minerals.

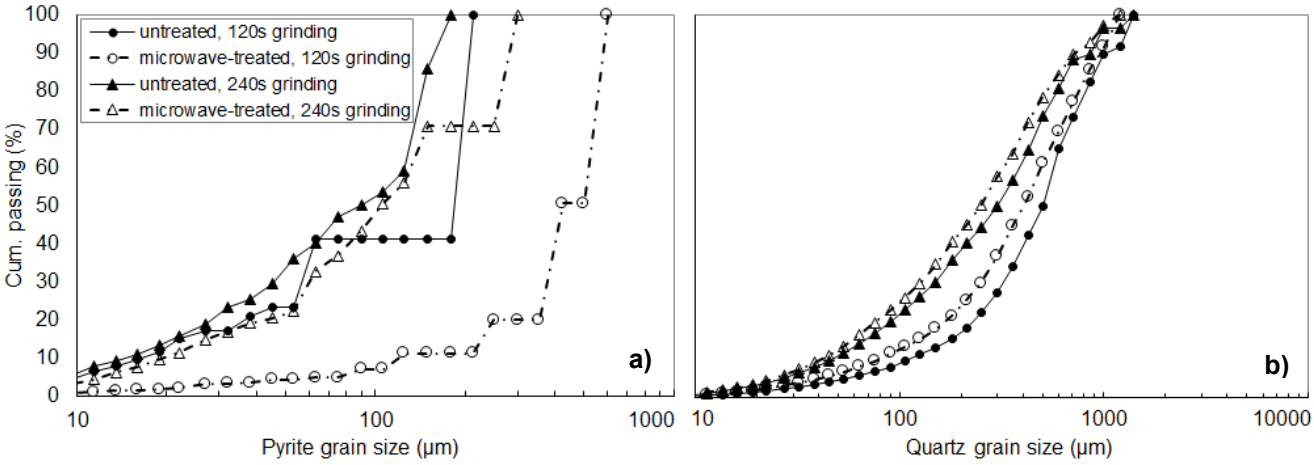

Figure 5. Grain size distribution of a) pyrite and b) quartz, at top size fraction -1600+1250 µm after 120 s and 240 s grinding time.

4.2. Comminution kinetics

Following the one-size fraction method and performing stepwise grinding at short interval times (10, 20, 40, 80, 120, and 240 s), the cumulative breakage distribution function (B_{ij}) for each comminution test is determined using the *BII* method (Eq. 8). The x-axis ranges from 0 to 1 and presents the relative reduction in size from two consecutive sieves, assuming the breakage function is normalized, meaning that it is independent of the starting top size fraction (Kelly and Spottiswood 1990). Figure 6 shows that the breakage function for every sample follows a similar trend, however, its values are dependent on the starting size fraction. Progeny particles originating from finer size fractions tend to break into relatively larger particles, whereas coarser size fractions break into smaller particles.

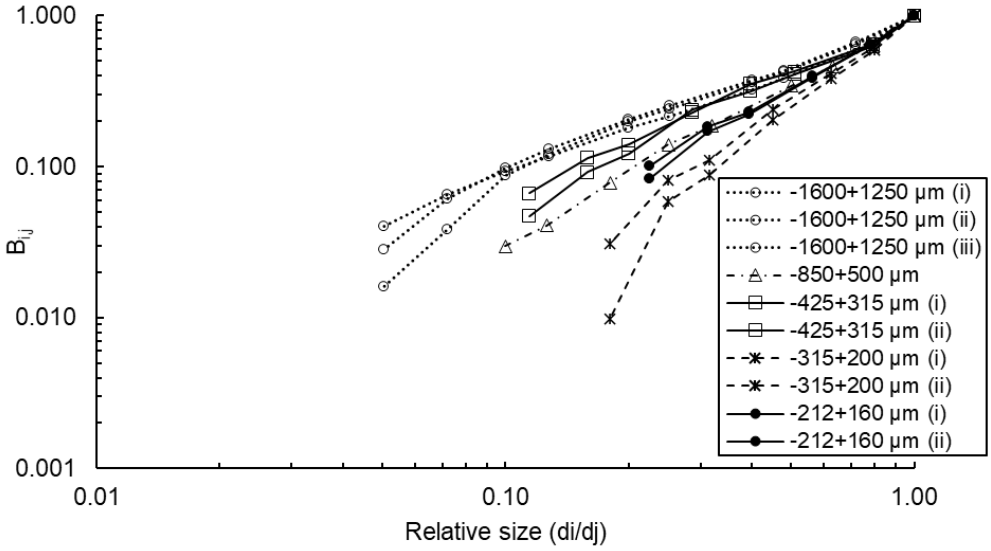

Figure 6. Cumulative breakage distribution function for untreated ore, after 240 s grinding time, for various size fractions: -1600+1250 µm, -850+500µm, -425+315 µm, -315+200 µm and -212+160 µm

A comparison of the effects of microwave treatment on the breakage distribution function is visualized in Figure 7, using the B_{ij} values for the top size fraction -425+315 µm. When the ore is subjected to microwave treatment, it tends to break into coarser particles, possibly indicating that breakage is occurring more frequently along grain boundaries when compared to the untreated samples.

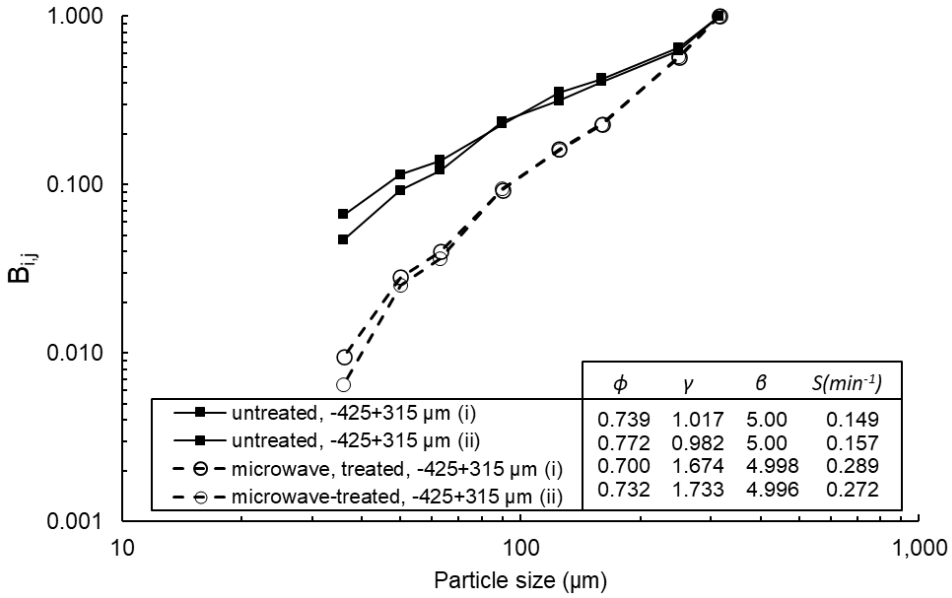

Figure 7. Breakage distribution function for microwave-treated and untreated samples. Top size fraction: -425+315 µm. Duplicate tests are presented

Fitting experimental data to Eq. 7, the breakage parameters ϕ, γ, and β were estimated (Figure 7) by solving a non-linear optimization algorithm in MATLAB (lsqcurvefit), minimizing the residual errors between experimental and predicted $B_{i,j}$ values.

The parameter γ (Eq. 7) determines the slope of the fine grinding term, meaning that as γ increases, the relevance of the fine grinding term in the equation diminishes and it generates fewer fines. For microwave-treated ore, γ is larger (see Figure 7) and represents an improvement as it avoids overgrinding, considering that the normalized grain size for sulfides is 298.81 µm and the generation of very fine particles is not required. Parameter ϕ confirms this affirmation, as it is directly related to the amount of fines generated after each primary breakage event. Therefore, Figure 7 shows an improvement in terms of liberation and breakage mechanism through grain boundary fracture when the ore is subjected to microwave treatment. This interpretation is in agreement with Kumar *et al*. (2010), as micro-cracks and fissures along grain boundaries were observed in an iron ore subjected to microwave treatment.

Additionally, the selection function (specific rate of breakage S_i) values are shown in Figure 7. The increase in S_i presents an improvement in grinding kinetics when microwave treatment is applied to the sample. For the size fractions ranging from 160 µm to 1250 µm (following the single-size fraction experiments as per Table 1), the specific rate of breakage curve is determined and visualized in Figure 8. It becomes clear that ore samples subjected to microwave-treatment have a greater breakage rate than the untreated ones.

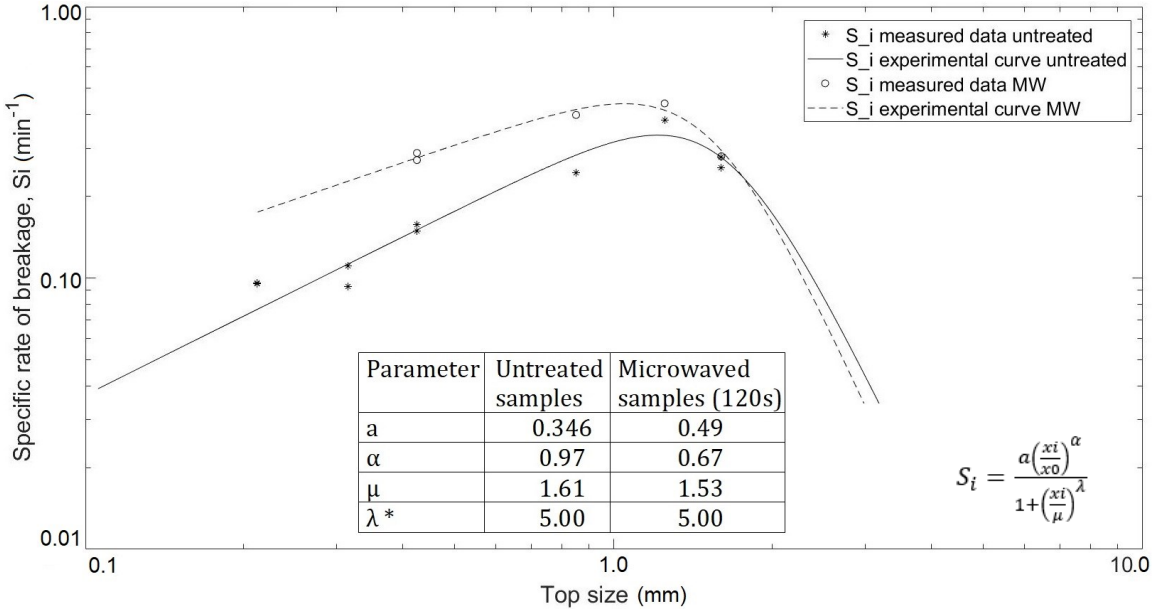

Figure 8. Specific rate of breakage for untreated and microwave-treated samples. (*) λ values are not deemed accurate as there is not enough data on coarser sizes to be able to quantify the deceleration rate

Fitting the specific breakage rate data to Eq. 10, following the model developed by Austin *et al*. (1984), the parameters for the specific rate of breakage are determined and listed within Figure 8. Note that due to the low number of sample data on coarser size fractions, the estimated λ values are not deemed accurate, as it overfits the data to decelerate breakage kinetics quickly enough to reach the only existing data point after the inflection point. Therefore, we should only focus on the parameters *a, α, and μ*.

The maximum rate of breakage for each experiment occurs at particle size close to the *μ* parameter, having similar values for both experiments. Microwave-treated samples show higher value for *a*, which is related to improvements in breakage rate constant. *α* is related to the kinetics at finer particle sizes, showing that microwave-treated samples grind faster at finer size fractions.

Microwave-treatment, therefore, is found to improve the size reduction, increase mineral liberation, and grinding kinetics, in agreement with other literature studies (Al-Harahsheh and Kingman 2004; Batchelor *et al*. 2016; Bobicki, Liu, and Xu 2018; Charikinya, Bradshaw, and Becker 2015; S. W. Kingman *et al*. 2004; Somani *et al*. 2017; Walkiewicz, Kazonich, and McGill 1988). However, when considering the energy consumption of microwave and grinding at a laboratory scale, it becomes clear that microwave consumes significantly higher amounts of energy and should, therefore, be applied for a minimal amount of time. For this work, the optimum microwave time has not been experimentally determined, but it is expected to be in the range from 60-90 s, as improvements are observed in terms of liberation and size reduction after 60 s exposure time (see Figure 3). Microcracks develop over time as microwaves preferentially interact with certain minerals and sufficient temperature-dependent tensions build up within the particles, leading to improvements in grinding performance.

Grinding a sample of 750 g from the studied ore consumes 8.1kWh/t per minute whereas microwave at the current settings of 1050W output power consumes 29.8 kWh/t per minute. For lab-scale studies, the energy consumption from microwave is too high compared to grinding energy, as a reduction in 5.5 minutes in grinding time would be required to break-even the energy consumption for 90 s microwave. However, the potential improvements at industrial scale should be further evaluated, as a reduction in the grinding time required to reach the target liberation characteristics might counterbalance the energy consumption from microwave, as per Bobicki *et al*. (2018).

4.3. Excess entropy analysis

The entropy analysis provides a local (for individual particles) and global (for streams) measure of process efficiency, as discussed by Buchmann *et al*. (2020) and Schach *et al*. (2019). It quantifies the intergrowth (liberation) and size distribution of the particles, looking at the molar concentration of each component (mineral group). The total chemical exergy of a stream, as calculated from Eq. 2, is an indication of the potential value to be extracted from each size fraction. If normalized by the mass, it provides an indication of the exergy concentration within particle size classes, representing a proxy for the surface area accessible for chemical exergy to be tapped from reactions in downstream processes (Figure 9). Thermodynamic relevant data for each mineral group in this work is presented in Table A. 1, in the appendix. Exergy calculations are already a standard metric for chemical separation processes and can be done easily in process flowsheet software, such as HSC Sim (Outotec 2020). The remaining challenge is to apply this concept to multicomponent particle-based systems, which is addressed in this work.

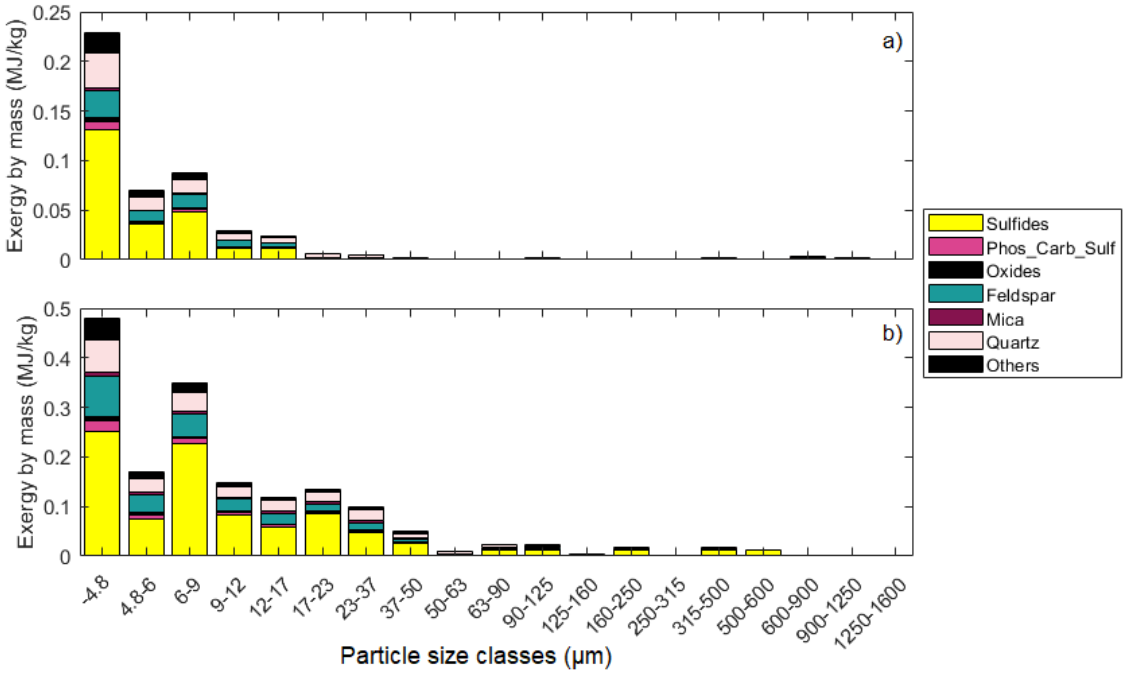

Figure 9. Exergy distribution for each size class, normalized by mass (kWh/kg), for a) untreated sample and b) Microwave-treated sample at 120 s grinding. The calculation is based on Eq. 2, considering every particle in the system. The yellow bars represent the specific exergy for the sulfide minerals

A comparison between untreated (Figure 9a) and microwave-treated (Figure 9b) experiments is made, showing the relatively higher distribution of exergy from the sulfide phases towards coarser size fractions. Despite microwave-treated samples having a slightly finer particle size distribution (see Figure 3), the exergy content of sulfide phases is less representative within the very fine particles (<4.8 µm) when microwave-treatment is applied, showing improvements in successfully liberating coarser sulfide grains. This can be better visualized using SEM (scanning electron microscopy) false-color images, as shown in Figure A. 2, in the appendix. It can be seen that the presence of liberated coarser sulfide particles is observed, in contrast to the untreated sample, which only contains liberated particles at finer particle sizes.

Figure 10 presents the exergy distribution within different liberation classes, calculated from Eq. 2, showing that for the microwave-treated samples (Figure 10b), the chemical exergy of sulfides available at liberated particles is higher than that of untreated samples (Figure 10a), which still has some exergy left into interlocked particles, as shown in the liberation class 10-20%, mostly.

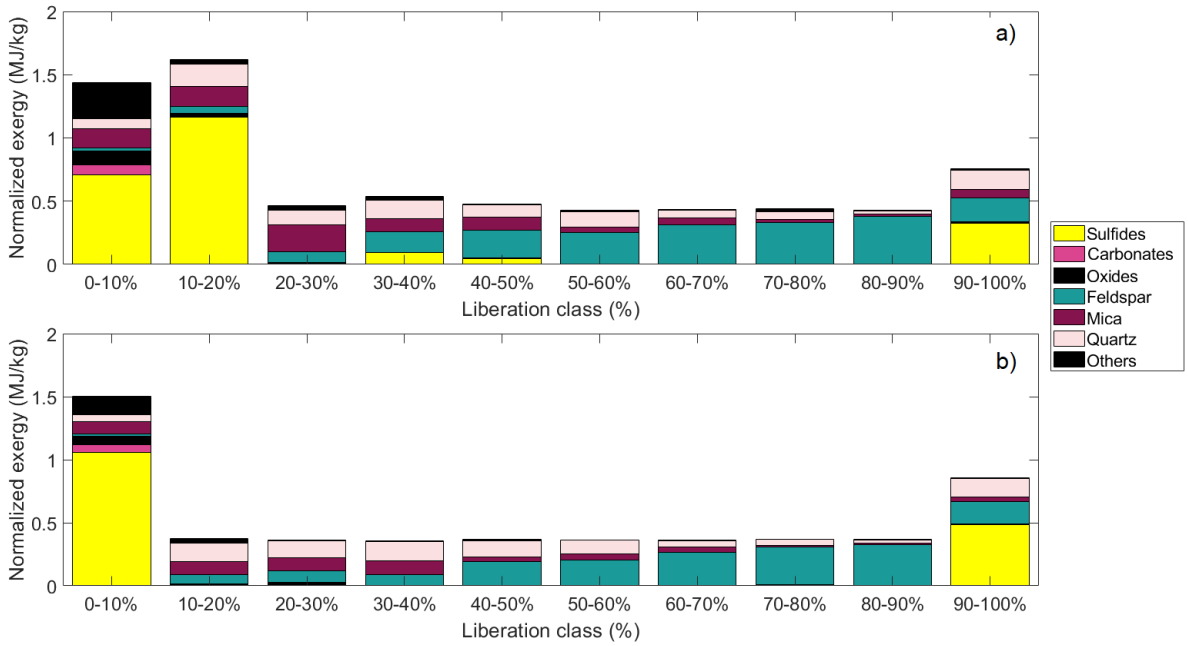

Figure 10. Normalized exergy distribution for each liberation class, split for each mineral component in the system. a) Untreated sample; b) Microwave-treated sample

Figure 10 shows that by introducing microwave-energy to the ore, a structural change occurs, which helps to concentrate the sulfides in the liberated classes. In terms of selectivity for grinding, the exergy content from sulfide minerals represents 42.98% in the liberated fraction (for untreated samples), whereas for microwave-treated samples this proportion rises to 56.90% of the exergy in liberated size fraction (90-100% liberation class). This result is observed despite the fact that both samples (untreated and microwave-treated) contain 70% of their sulfide particles in the liberated class (Figure A. 3). It means that microwave treatment liberates particles at coarser sizes, having higher exergy content in the liberated size fractions when compared to the untreated samples. Exergy, therefore, presents itself as a combined metric of mineral liberation and particle size.

The excess entropy method is another measure of the combined effects of size reduction and liberation (Peuker *et al*. 2021). As grinding time increases, the particle size becomes finer (up to a certain limit) and mineral phases are more liberated. Looking at a global level (streams), smaller particles increase the overall amount of permutations in a particle bed. When looking at a local level (individual particles), the molar excess entropy factor, as per Eq. 5, becomes a measure of the structure of the particles in the system, representing the mixing at the micro-scale.

The composition of the particles can be described by the molar intergrowth ratio (IGR), representing the ratio of moles within locked particles to the overall moles in the system:

$$IGR = \frac{\Sigma_j n_j}{n} \qquad (11)$$

The IGR is a combination of the locked particles from different components in the mixture (7 mineral groups, as described in Table A. 1, in the appendix) and represents the overall liberation of the sample. Figure 11 presents the excess entropy factor for different grinding times, thus varying the IGR.

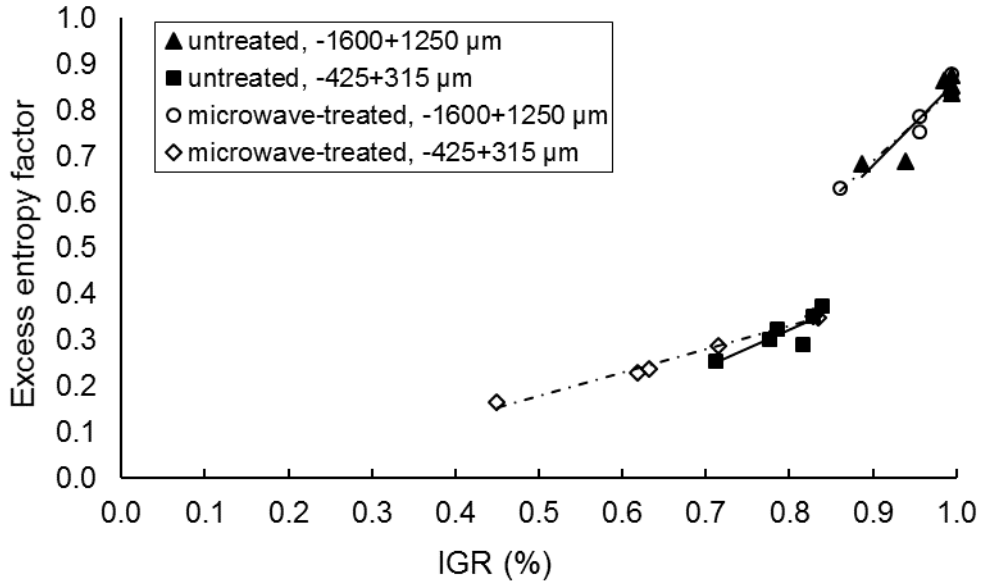

Figure 11. Excess entropy factor ($\frac{S^x}{k}$) at different particle intergrowth ratio (IGR), for multicomponent systems. Lines are used to guide the eye towards a general trend

Figure 11 shows the excess entropy relationship to liberation and particle size, calculated from particle data originated from four sets of experiments: at two different size fractions, with and without microwave-treatment. It demonstrates that the higher the intergrowth ratio, the greater is the excess entropy. For a binary system, this can be easily visualized in Figure A. 4, in the appendix, showing that the highest entropy is found for a 50% molar concentration of the component of interest. Additionally, we observe that the smaller the mass (molarity) of a particle, the smaller the absolute excess entropy factor becomes.

However, the excess entropy alone cannot show a clear dependency on particle size. For the experiments on the coarse size fraction (-1600+1250 µm), for instance, there is a change in particle size (as seen Figure A. 1, in the appendix) when microwave-treatment is applied to the sample, however, the excess entropy remains unchanged when compared to the untreated samples (Figure 11). For the fine size fraction, we observe that the shift in excess entropy from both experiments is mostly governed by improvements in liberation.

It can be concluded that both the excess entropy method and the exergy analysis are capable of addressing changes in mineral liberation (Figure 4) and size reduction. An inverse correlation between the excess entropy factor and the exergy available in liberated particles (liberation degree higher than 90%) is observed in Figure 12. With an increase in liberation, the system becomes less chaotic, hence decreasing the excess entropy and increasing the exergy in liberated particles, which also represents a separation effect.

As grinding takes place, there is an increase in the exergy content available to be tapped from higher liberation classes, with a consequent reduction in the excess entropy within locked particles. For microwave-treated samples, the excess entropy within locked particles is smaller for similar liberation characteristics, showing improvements as microwave treatment is used for assisting comminution.

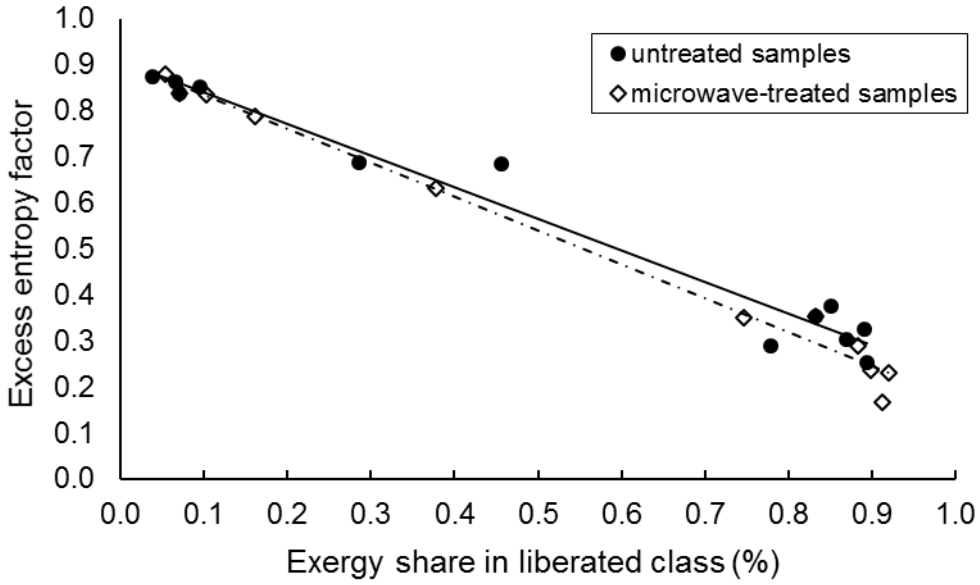

Figure 12. Exergy in liberation particles versus excess entropy factor. The exergy value shown represents the share of exergy content that is available in particles with over 90% liberation.

5. Conclusions

This paper has applied the exergy analysis and excess entropy method on two sets of experiments related to the microwave-treatment of a gold-copper ore. This methodology is based on the approach for ideal mixing on the particle level for multicomponent systems, using automated mineralogy data to quantify the entropy of intergrown particles as grinding occurs. This is a first step towards understanding mineral processing not only in terms of energy conservation (first law of thermodynamics) but also looking at the quality of energy available at multicomponent systems (second law of thermodynamics).

Current studies only analyze the effects of the ideal mixing entropy in separation processes, which is not sufficient to describe a multicomponent particle-based system. The introduction of an excess entropy term for interlocked particles addresses such complex particle texture. It enables us to understand the change in particle composition and its degree of liberation, as well as changes in particle size during comminution, being an important measure of process efficiency and selectivity.

Microwave-assisted grinding was evaluated using traditional approaches, looking at particle size reduction and understanding the liberation characteristics of the ore. Improvements in breakage kinetics and liberation are observed, however, energy consumption still poses a challenge for the application. A more detailed analysis is carried out, looking at the exergy distribution towards different particle sizes and liberation classes. The normalized exergy distribution is also a combined measure for both effects taking place during comminution, i.e. changes in particle size and liberation. It shows that microwave-treatment tends to increase the exergy content of the mineral of interest (pyrite) in liberated size fractions, which represents an improvement as coarser particles are liberated when microwave-treatment is used.

Further studies are required to understand the entropy effects in a beneficiation flowsheet comprised of several mineral processing unit operations, looking at improvements in comminution and its effects further downstream in separation processes. Process simulation tools and flowsheeting are a great way of understanding the exergy distribution as physical and chemical processes occur, and evaluate optimum processes based on the concept of maximizing the specific exergy available in concentrate streams. With the help of such simulation tools, sufficient experimental data can be generated for estimating the entropy creation factor Ł.

Further studies are aimed at understanding the applicability of the exergetic analysis and excess entropy methods to identify and quantify the occurrence of different breakage mechanisms (intergranular versus transgranular), based on the principle of maximum entropy and trying to identify breakage paths that result in minimum exergy losses.

The entropy analysis for multicomponent particle-based systems is proposed to become a standard in mineral processing analyses, helping quantify and connect physical processes and chemical reactions, bridging the knowledge gap between minerals processing and metallurgy experts. Particle-based systems can be seen as a collection of interlocked “molecules” and hence, the second law of thermodynamics should be used as a measure of process efficiency that correlates and interprets the state of mixing of particle texture and homogeneous liquid mixtures.

Acknowledgments

The authors would like to thank Dr. Thomas Mütze and Dr. Thomas Leißner for their support and for granting permission to use the laboratory infrastructure from the Institute of Mechanical Process Engineering and Mineral Processing, TU Bergakademie Freiberg. We thank Dr. Alphonce Wikedzi for collecting the samples, and Dr. Duong Hoang for the fruitful discussions for designing the experiments.

This paper is dedicated to the memory of Omar Velázquez-Martinez who sadly passed away at young age just when this paper was first submitted. Without his pioneering contributions, this paper surely would not have been possible.

References

Abadias Llamas, A., A. Valero Delgado, A. Valero Capilla, C. Torres Cuadra, M. Hultgren, M. Peltomäki, A. Roine, M. Stelter, and M. A. Reuter. 2019. “Simulation-Based Exergy, Thermo-Economic and Environmental Footprint Analysis of Primary Copper Production.” *Minerals Engineering* 131:51–65.

Adewuyi, Sefiu O., Hussin A. M. Ahmed, and Haitham M. A. Ahmed. 2020. “Methods of Ore Pretreatment for Comminution Energy Reduction.” *Minerals* 10(5):423.

Al-Harahsheh, M. and S. W. Kingman. 2004. “Microwave-Assisted Leaching - A Review.” *Hydrometallurgy* 73(3–4):189–203.

Amini, S. H., J. A. M. Remmerswaal, M. B. Castro, and M. A. Reuter. 2007. “Quantifying the Quality Loss and Resource Efficiency of Recycling by Means of Exergy Analysis.” *Journal of Cleaner Production* 15(10):907–13.

Austin, L. G., R. R. Klimpel, and P. T. Luckie. 1984. *Process Engineering of Size Reduction: Ball Milling*. edited by SME. New York.

Austin, L. G. and P. T. Luckie. 1972. “Methods for Determination of Breakage Distribution Parameters.” *Powder Technology* 5(4):215–22.

Bachmann, Kai, Max Frenzel, Joachim Krause, and Jens Gutzmer. 2017. “Advanced Identification and Quantification of In-Bearing Minerals by Scanning Electron Microscope-Based Image Analysis.” *Microscopy and Microanalysis* 23(3):527–37.

Ballantyne, G. R. and M. S. Powell. 2014. “Benchmarking Comminution Energy Consumption for the Processing of Copper and Gold Ores.” *Minerals Engineering* 65:109–14.

Batchelor, A. R., D. A. Jones, S. Plint, and S. W. Kingman. 2015. “Deriving the Ideal Ore Texture for Microwave Treatment of Metalliferous Ores.” *Minerals Engineering* 84:116–29.

Batchelor, A. R., D. A. Jones, S. Plint, and S. W. Kingman. 2016. “Increasing the Grind Size for Effective Liberation and Flotation of a Porphyry Copper Ore by Microwave Treatment.” *Minerals Engineering* 94:61–75.

Bobicki, E. R., D. Boucher, J. Forster, A. Gillis, G. Holcroft, D. Fragomeni, E. Whiteman, C. Pickles, and A. Olmsted. 2020. “CANMICRO: SCALING UP MICROWAVE TECHNOLOGY FOR THE MINING INDUSTRY.” Pp. 131–44 in *52nd Annual Canadian Mineral Processors Operators Conference*. Vol. 52. Otawa, Canada.

Bobicki, Erin R., Qingxia Liu, and Zhenghe Xu. 2014. “Microwave Heating of Ultramafic Nickel Ores and Mineralogical Effects.” *Minerals Engineering* 58:22–25.

Bobicki, Erin R., Qingxia Liu, and Zhenghe Xu. 2018. “Microwave Treatment of Ultramafic Nickel Ores: Heating Behavior, Mineralogy, and Comminution Effects.” *Minerals* 8(11):1–19.

Buchmann, Markus, Edgar Schach, Thomas Leißner, Marius Kern, Thomas Mütze, Martin Rudolph, Urs A. Peuker, and Raimon Tolosana-Delgado. 2020. “Multidimensional Characterization of Separation Processes – Part 2: Comparability of Separation Efficiency.” *Minerals Engineering* 150:106284.

Cao, Wenbin. 2012. *The Development and Application of Microwave Heating*. InTech.

Charikinya, E., S. Bradshaw, and M. Becker. 2015. “Characterising and Quantifying Microwave Induced Damage in Coarse Sphalerite Ore Particles.” *Minerals Engineering* 82:14–24.

Curry, James A., Mansel J. L. Ismay, and Graeme J. Jameson. 2014. “Mine Operating Costs and the Potential Impacts of Energy and Grinding.” *Minerals Engineering* 56:70–80.

Fandrich, Rolf, Ying Gu, Debra Burrows, and Kurt Moeller. 2007. “Modern SEM-Based Mineral Liberation Analysis.” *International Journal of Mineral Processing* 84(1–4):310–20.

Fernandes, I. B., A. Abadías Llamas, and M. A. Reuter. 2020. “Simulation-Based Exergetic Analysis of NdFeB Permanent Magnet Production to Understand Large Systems.” *Jom* 72(7):2754–69.

Gay, S. L. 2004. “A Liberation Model for Comminution Based on Probability Theory.” *Minerals Engineering* 17(4):525–34.

Gholami, Hamed, Bahram Rezai, Ahmad Hassanzadeh, Akbar Mehdilo, and Majid Behjat Jabbari. 2020a. “The Effect of Microwave’s Location in a Comminution Circuit on Improving Grindability of a Porphyry Copper Deposit.” *Energy Sources, Part A: Recovery, Utilization, and Environmental Effects* 1–20.

Gholami, Hamed, Bahram Rezai, Akbar Mehdilo, Ahmad Hassanzadeh, and Mohammadreza Yarahmadi. 2020b. “Effect of Microwave System Location on Floatability of Chalcopyrite and Pyrite in a Copper Ore Processing Circuit.” *Physicochemical Problems of Mineral Processing* 56(3):432–48.

Haque, Kazi E. 1999. “Microwave Energy for Mineral Treatment Processes - A Brief Review.” *International Journal of Mineral Processing* 57(1):1–24.

Heinig, T., K. Bachmann, R. Tolosana-Delgado, G. Van Den Boogaart, and J. Gutzmer. 2015. “Monitoring Gravitational and Particle Shape Settling Effects on MLA Sampling Preparation.” Pp. 200–206 in *Proceedings of IAMG 2015 - 17th Annual Conference of the International Association for Mathematical Geosciences*.

Herbst, John A. 1979. “Rate Processes in Multiparticle Metallurgical Systems.” Pp. 53–112 in *Rate Processes of Extractive Metallurgy*, edited by H. Y. Sohn and M. E. Wadsworth. Salt Lake City.

Ignatenko, O., A. van Schaik, and M. A. Reuter. 2007. “Exergy as a Tool for Evaluation of the

Resource Efficiency of Recycling Systems." *Minerals Engineering* 20(9):862–74.

Jinkai, Xiao. 1990. "Dielectric Properties of Minerals and Their Applications in Microwave Remote Sensing." *Chinese Journal of Geochemistry* 9(2):169–77.

John, R. S., A. R. Batchelor, D. Ivanov, O. B. Udoudo, D. A. Jones, C. Dodds, and S. W. Kingman. 2015. "Understanding Microwave Induced Sorting of Porphyry Copper Ores." *Minerals Engineering* 84:77–87.

Kelly, E. G. and D. J. Spottiswood. 1990. "The Breakage Function; What Is It Really?" *Minerals Engineering* 3(5):405–14.

Kingman, S.W., K. Jackson, S. M. Bradshaw, N. A. Rowson, and R. Greenwood. 2004. "An Investigation into the Influence of Microwave Treatment on Mineral Ore Comminution." *Powder Technology* 146(3):176–84.

Kingman, S. W., K. Jackson, A. Cumbane, S. M. Bradshaw, N. A. Rowson, and R. Greenwood. 2004. "Recent Developments in Microwave-Assisted Comminution." *International Journal of Mineral Processing* 74(1–4):71–83.

Kumar, P., B. K. Sahoo, S. De, D. D. Kar, S. Chakraborty, and B. C. Meikap. 2010. "Iron Ore Grindability Improvement by Microwave Pre-Treatment." *Journal of Industrial and Engineering Chemistry* 16(5):805–12.

Leißner, T., D. H. Hoang, M. Rudolph, T. Heinig, K. Bachmann, J. Gutzmer, H. Schubert, and U. A. Peuker. 2016. "A Mineral Liberation Study of Grain Boundary Fracture Based on Measurements of the Surface Exposure after Milling." *International Journal of Mineral Processing* 156:3–13.

Little, Lucy, Aubrey N. Mainza, Megan Becker, and Jenny G. Wiese. 2016. "Using Mineralogical and Particle Shape Analysis to Investigate Enhanced Mineral Liberation through Phase Boundary Fracture." *Powder Technology* 301:794–804.

Lu, Gao ming, Yuan hui Li, Ferri Hassani, and Xiwei Zhang. 2017. "The Influence of Microwave Irradiation on Thermal Properties of Main Rock-Forming Minerals." *Applied Thermal Engineering* 112:1523–32.

Meskers, C. E. M., M. A. Reuter, U. Boin, and A. Kvithyld. 2008. "A Fundamental Metric for Metal Recycling Applied to Coated Magnesium." *Metallurgical and Materials Transactions B: Process Metallurgy and Materials Processing Science* 39(3):500–517.

Outotec. 2020. "HSC Sim: Process Simulation Module from HSC Chemistry." Retrieved (https://www.outotec.com/products-and-services/technologies/digital-solutions/hsc-chemistry/hsc-sim-process-simulation-module/).

Peuker, U., M. Reuter, G. Van Den Boogaart, M. Rudolph, and R. Tolosana-delgado. 2021. "The Entropy of Intergrown Particle Mixtures - a Contribution to Holistic Flowsheet Simulation." Pp. 18–22 in *XXX International Mineral Processing Congress*.

Schach, Edgar, Markus Buchmann, Raimon Tolosana-Delgado, Thomas Leißner, Marius Kern, K. Gerald van den Boogaart, Martin Rudolph, and Urs A. Peuker. 2019. "Multidimensional Characterization of Separation Processes – Part 1: Introducing Kernel Methods and Entropy in the Context of Mineral Processing Using SEM-Based Image Analysis." *Minerals Engineering* 137(November 2018):78–86.

Somani, Aditya, Tapas K. Nandi, Samir K. Pal, and Arun K. Majumder. 2017. "Pre-Treatment of Rocks Prior to Comminution – A Critical Review of Present Practices." *International Journal of Mining Science and Technology* 27(2):339–48.

Szargut, J. 1989. "Chemical Exergies of the Elements." *Applied Energy* 32(4):269–86.

Velázquez Martínez, O., K. G. Van Den Boogaart, M. Lundström, A. Santasalo-Aarnio, M.

Reuter, and R. Serna-Guerrero. 2019. “Statistical Entropy Analysis as Tool for Circular Economy: Proof of Concept by Optimizing a Lithium-Ion Battery Waste Sieving System.” *Journal of Cleaner Production* 212:1568–79.

Walkiewicz, J. W., G. Kazonich, and S. L. McGill. 1988. “Microwave Heating Characteristics of Selected Minerals and Compounds.” *Mineral and Metallurgical Processing* (5(1)):39–42.

Wang, Ge, Peter Radziszewski, and Jacques Ouellet. 2008. “Particle Modeling Simulation of Thermal Effects on Ore Breakage.” *Computational Materials Science* 43(4):892–901.

Wikedzi, A., M. A. Arinanda, T. Leißner, U. A. Peuker, and T. Mütze. 2018. “Breakage and Liberation Characteristics of Low Grade Sulphide Gold Ore Blends.” *Minerals Engineering* 115:33–40.

Wikedzi, A., S. Saquran, T. Leißner, U. A. Peuker, and T. Mütze. 2020. “Breakage Characterization of Gold Ore Components.” *Minerals Engineering* 151:106314.

Wikedzi, Alphonce Wendelin. 2018. “Optimization and Performance of Grinding Circuits : The Case of Buzwagi Gold Mine (BGM).” Technische Universität Bergakademie Freiberg.

Wong, D. 1975. “Microwave Dielectric Constants of Metal Oxides at High Temperature.” University of Alberta, Canada.

Appendix

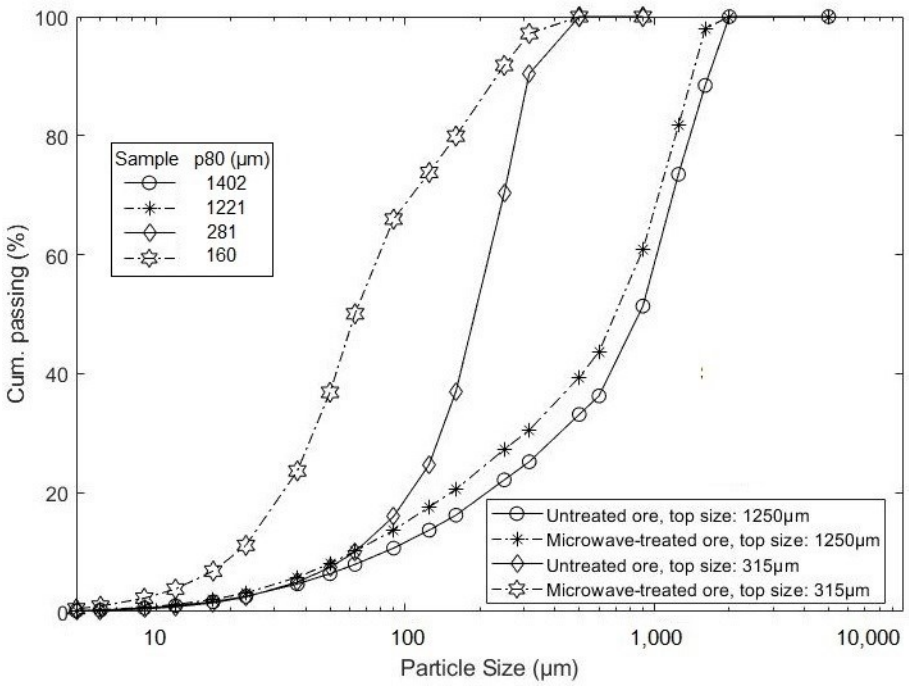

Figure A. 1. Cumulative particle size distribution after 240 s grinding for microwave treated (120 s) and untreated ore, from top size fraction experiments -1600+1250 µm and -425+315 µm, obtained from automated mineralogy data

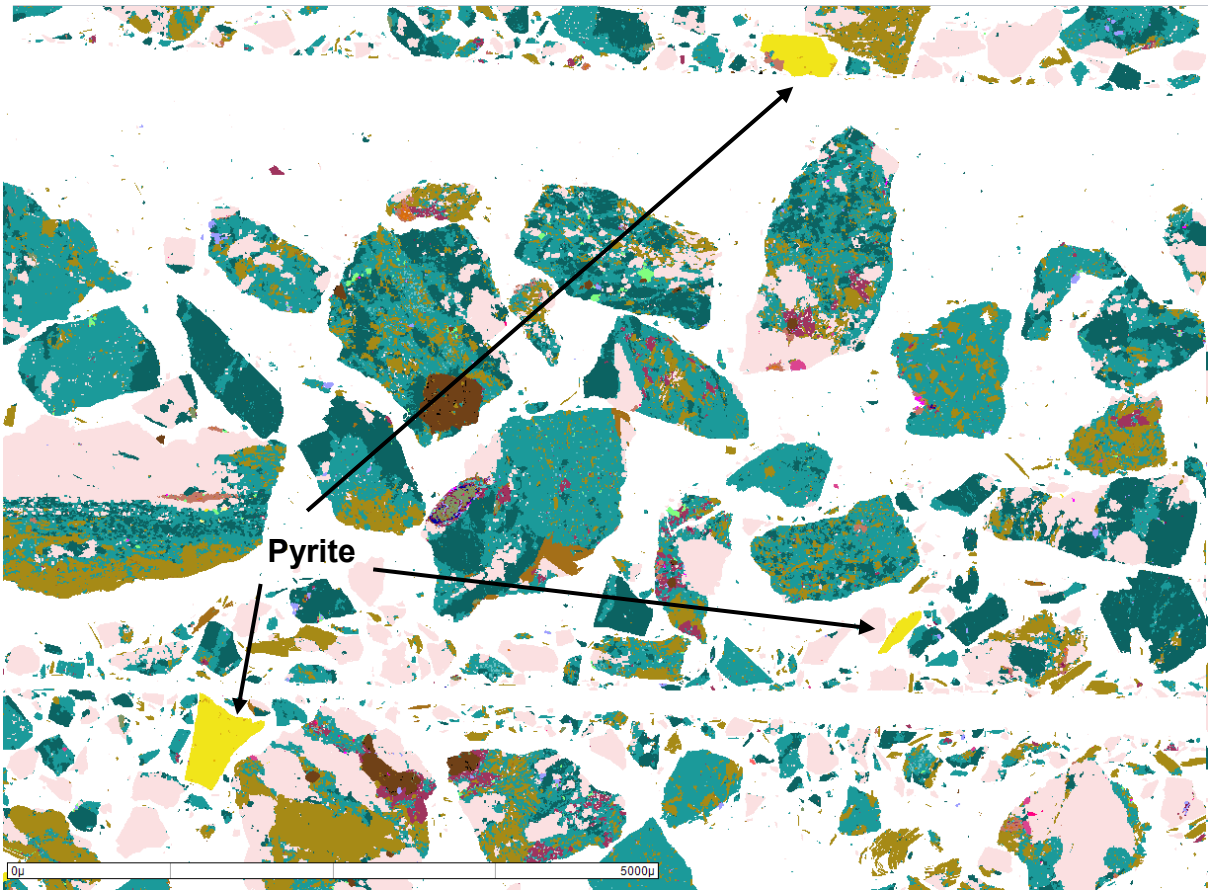

Figure A. 2. False-color image after 120 s grinding time, showing some coarse liberated pyrite. The same effect is not observed for the untreated samples

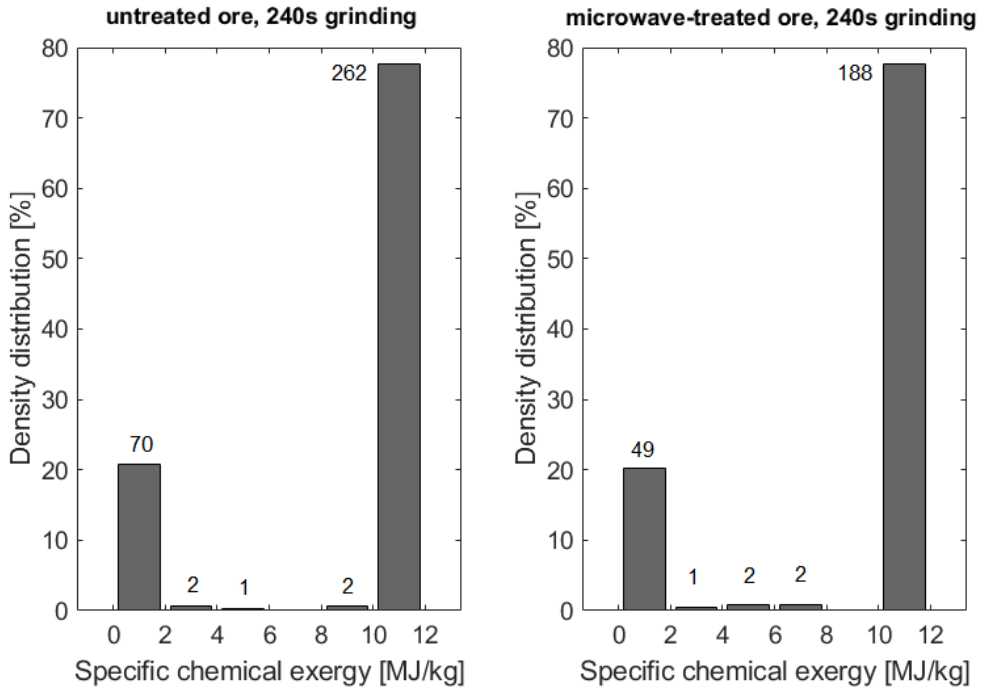

Figure A. 3. Density distribution function for chemical exergy on particles containing sulfide minerals. The higher the liberation in a particle, the closer the specific chemical exergy gets to the target mineral (for pyrite, this represents 11.94 MJ/kg, as seen in Table A.1. The labels represent the total number of particles in each class.

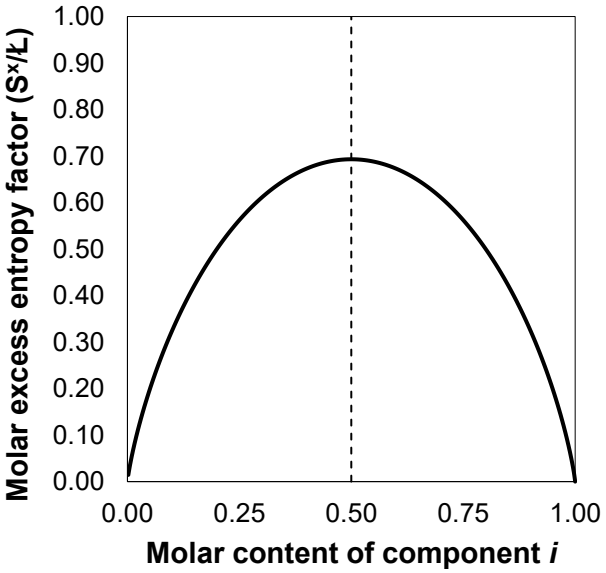

Figure A. 4. Molar excess entropy factor for a binary system. The highest entropy is observed for a molar concentration of 50% in a particle

Table A. 1. Thermodynamic data on the mineral groups used in this study. Obtained from HSC Chemistry's database (Outotec 2020) *and website: http://web.mit.edu/2.813/www/readings/APPENDIX.pdf*

Mineral group	**Main mineral**	**Chemical composition**	**Molecular Weight (g/mol)**	**Standard enthalpy of formation ΔH˚f (kJ/mol)**	**Standard chemical exergy e^0_i (kJ/mol)**	**Specific chemical exergy (kJ/kg)**
Sulfides	Pyrite	FeS_2	119.98	-167.36	1,432.73	11941.95
Carbonates	Calcite	$CaCO_3$	100.09	-1,207.10	17.16	171.51
Oxides	Hematite	Fe_2O_3	159.69	-825.50	11.65	72.98
Feldspars	Albite + Orthoclase	$NaAlSi_3O_8$ + $KAlSi_3O_8$	270.28	-3,944.08	5.82	21.55
Micas	Muscovite	$KAl_2(AlSi_3O_{10})(OH)_2$	398.31	-5,976.56	1.72	4.31
Quartz	Quartz	SiO_2	60.08	-910.86	2.48	41.23
Others	Epidote	$Ca_2FeAl_2Si_3O_{12}OH$	483.22	-6,461.90	57.02	118.00